COL6A3 Exosomes Promoting Tumor Dissemination and Metastasis in Epithelial Ovarian Cancer

Chih-Ming Ho *, Ting-Lin Yen, Tzu-Hao Chang, Shih-Hung Huang

Posted Date: 18 June 2024

doi: 10.20944/preprints202406.1228.v1

Keywords: exosomes; COL6A3; metastasis; epithelial ovarian cancer; aggressiveness; exosomes inhibitor

Article

COL6A3 Exosomes Promoting Tumor Dissemination and Metastasis in Epithelial Ovarian Cancer

Chih-Ming Ho [1,2,3]*, Ting-Lin Yen [3,4], Tzu-Hao Chang [5] and Shih-Hung Huang [6]

[1] Gynecologic Cancer Center, Department of Obstetrics and Gynecology, Cathay General Hospital, Taipei, Taiwan; cmho@cgh.org.tw
[2] School of Medicine, Fu Jen Catholic University, Hsinchuang, New Taipei City, Taiwan
[3] Department of Medical Research, Cathay General Hospital, Sijhih, New Taipei City, Taiwan
[4] School of Medicine, Taipei Medical University, Taipei, Taiwan; d119096015@tmu.edu.tw
[5] Graduate Institute of Biomedical Informatics, Taipei Medical University, Taipei, Taiwan; kevin chang@tmu.edu.tw
[6] Department of Pathology Cathay General Hospital, Taipei, Taiwan; a68@cgh.org.tw
* Correspondence: cmho@cgh.org.tw; Tel: +886-2-27082121-1081

Abstract: Our study explores the role of cancer-derived extracellular exosomes (EXs), particularly focusing on collagen alpha-3 (VI; COL6A3), in facilitating tumor dissemination and metastasis in epithelial ovarian cancer (EOC). We found that COL6A3 is expressed in aggressive ES2 derivatives, SKOV3 overexpressing COL6A3 (SKOV3/COL6A3), and mesenchymal-type ovarian carcinoma stromal progenitor cells (MSC-OCSPCs), as well as their EXs, but not in less aggressive SKOV3 cells or ES2 cells with COL6A3 knockdown (ES2/shCOL6A3). High COL6A3 expression correlates with worse overall survival in EOC patients, as evidenced by TCGA and GEO data analysis. In vitro experiments showed that EXs from MSC-OCSPCs or SKOV3/COL6A3 cells significantly enhance invasion ability in ES2 or SKOV3/COL6A3 cells, respectively (both, P <0.001). In contrast, ES2 cells with ES2/shCOL6A3 EXs exhibit reduced invasion ability (p<0.001). In vivo, the average disseminated tumor numbers in the peritoneal cavity were significantly greater in mice receiving intraperitoneally injected SKOV3/COL6A3 cells than in SKOV3 cells (p<0.001). Furthermore, mice intravenously (IV) injected with SKOV3/COL6A3 cells and SKOV3/COL6A3-EXs showed increased lung colonization compared to mice injected with SKOV3 cells and PBS (p=0.007) or SKOV3/COL6A3 cells and PBS (p=0.039). Knockdown of COL6A3 or treatment with EXs inhibitor GW4869 or rapamycin-abolished COL6A3-EXs may suppress the aggressiveness in EOC.

Keywords: exosomes; COL6A3; metastasis; epithelial ovarian cancer; aggressiveness; exosomes inhibitor

1. Introduction

Ovarian cancer has the highest mortality rate among gynecological cancers [1]. Due to the lack of obvious symptoms and effective screening methods, most patients are diagnosed at an advanced stage, and surgery is unable to remove all tumors, resulting in a poor prognosis [2]. Advanced epithelial ovarian cancer (EOC) has widespread dissemination in the abdominal cavity with residual tumors after debulking surgery and resistance to chemotherapy drugs [3–5]. EOC metastasis is mainly through peritoneal dissemination. At least one-third of patients with EOC develop ascites with a poor prognosis, in which their five-year survival declines sharply [6].

Recent studies have indicated that cancer cells secrete extracellular vesicles (EVs), promoting cancer invasion, dissemination, and development in a cancer microenvironment [7]. EVs include exosomes (EXs) and microvesicles, which are small membrane vesicles containing microRNAs (miRNAs), messenger RNAs, and proteins [8,9]. EXs are small vesicles of ~30–150 nm in size, developed within endosomes through membrane invaginations [8]. The cancer-derived EXs

 doi:10.20944/preprints202406.1228.v1

participated in the promoting dissemination and metastasis from the initial stages to the development of secondary tumors [10–13]. EXs possess several unique advantages as biomarkers for the early detection of dissemination, because they are stable, abundant, and tumor-specific, and can be detected in the blood or ascites [9]. Recent evidence has demonstrated that cancer cell EXs affect both autocrine cancer cells and paracrine on the microenvironment. A previous study indicated ovarian cancer EXs could transfer CD44 to the peritoneal mesothelium to invade the physical barrier 14]. Ascites-derived EXs from ovarian cancer patients bring MMP1 mRNA and induce apoptosis in mesothelial cells [15]. EXs released from EOC cells promote and shift the conversion from normal fibroblasts and adipose-derived mesenchymal stem cells to cancer-associated fibroblasts (CAFs) [16,17]), and activated mesenchymal phenotype [18]. EOC primary tumors can create an advantageous microenvironment to help tumor attachment in distant organs through malignant ascites-derived EXs, which are dynamic remodeling tumor stroma and forming metastatic niches in the omentum from the CAF conversion [19].

Collagen type II secreted from stromal fibroblasts may promote tumor growth and angiogenesis [20], meanwhile, collagen type VI secreted from the base membrane, directly affects tumor growth, invasion, and metastasis in various neoplasms [21]. Our previous study demonstrated that upregulation of collagen type VI α3 (COL6A3) may promote tumor invasion and metastasis in EOC [22]. Furthermore, COL6A3 has been reported to be associated with cisplatin resistance in an autocrine manner [23]. A recent study disclosed that chemotherapy upregulated the expression of collagen type VI in the omentum and peritoneum of EOC [24]. COL6 is primarily derived from the tumor stroma, and increased COL6 gene expression in solid tumors is associated with shortened progression-free intervals and survival [25].

The EXs from more aggressive EOC cells strongly enhance aggressive behavior in less aggressive tumors, which promote aggressiveness without changing the properties of EOC cells from non-aggressive to aggressiveness [15]. To further investigate which components mainly affect aggressiveness underlying EXs from more aggressive ovarian cancer cells and in the microenvironment of ascites, we used ES2 cell line as a more aggressive phenotype exhibiting **fibroblast-like morphology** that was isolated from the ovary of a female human with clear cell carcinoma, and SKOV3 cell line as a less aggressive phenotype exhibiting epithelial-like morphology that was derived from the ascites of a female human with serous cystadenocarcinoma. Our recent study showed COL6A3 could be detected in culture medium and is abundant in primary ovarian cancer tissues, disseminated metastatic omentum tissues, EOC spheroids, and MSC-OCSPCs appear to process the new function of promoting EOC in EMT, stemness, tumor growth, and metastasis [22]. COL6A3 belongs to an extracellular matrix (ECM) gene and is classified as a mesenchymal type associated gene, which was the worst prognosis subtype in EOC from TCGA molecular subtype analyses [22].

In this study, we elucidated for the first time COL6A3 transport via EXs from EOC and MSC-OCSPCs conferring invasiveness and metastasis in EOC cells. We evaluated treatment strategies focusing on lysosomes, autophagy inhibition, and possible target genes on EOC cells and EXs in vitro experiments and in vivo live mouse models.

2. Results

2.1. Characterization of Exosomes in EOC and Ascites-Derived Cell Lines

We first characterized the particle size of exosomes (EXs) from more aggressive ES2 cells, ES2 paclitaxel-resistant cells (ES2TR), ES2-derived tumor spheres (ES2 TS), and ES2 paclitaxel-resistant cells derived tumor spheres (ES2TR TS), which have been established in our lab as previously described [22]. Using nanoparticle tracking analysis, the mean particle size of ES2 EXs, ES2TR EXs, ES2 TS EXs, and ES2TR TS EXs was 102 nm, 96.8 nm, 134 nm, and 132 nm, respectively. The mean concentration of the number of particles (x 10^6/ml) of ES2 EXs, ES2TR EXs, ES2 TS EXs, and ES2TR TS EXs was 4.8, 7.3, 2.8, and 2.8, respectively. The percentages of pluripotent factors and drug resistance-related factors were substantially higher in ES2 TS and ES2TR160 TS than in ES2 and ES2

 doi:10.20944/preprints202406.1228.v1

TR160, respectively, by flow cytometric analysis [28]. Two morphologically different adherent cell populations of ovarian cancer stromal progenitor cells (OCSPCs) from two EOC patients' ascites and tissues were cultured and isolated in selective conditional media [26] (Figure 1(a) right panel). Epithelial-like OCSPCs (epi-OCSPCs) promoted tumorigenesis, in contrast, mesenchymal-like OCSPCs (MSC-OCSPCs) enhanced the migration, invasion, and spheroid aggregation of EOC [29]. High expression of vimentin with low expression of CK18 and E-cadherin in MSC-OCSPCs; in contrast, low expression of vimentin with high expression of CK18 and E-cadherin in epi-OCSPCs were characteristic in two types of cells (Figure 1(a) left upper panel). The high CD133, CD117, SSEA4, and CA125 expression in epi-OCSPCs and MSC-OCSPCs revealed OCSPCs processed stemness characteristics and malignant change (Figure 1(a) left lower panel). We further characterized the particle size of ascites-derived EXs using nanoparticle tracking analysis. The mean particle size of ascites-derived EXs from 2 advanced EOC patients was 100 nm and 94 nm, respectively. The mean concentration of ascites-derived EX particles (x 10^{10}/ml) was 4.5 and 3.93, respectively, and suggested ascites contained abundant EX particles. The consistent expression of positive stemness surface expression markers of CD133, CD117, and CD34 by flow cytometry in EOC cells and MSC-OCSPCs, and those derived EXs revealed EOC cells and MSC-OCSPCs-derived EXs processed stemness characteristics as well as EOC cells and MSC-OCSPCs (Figure 1(b)).

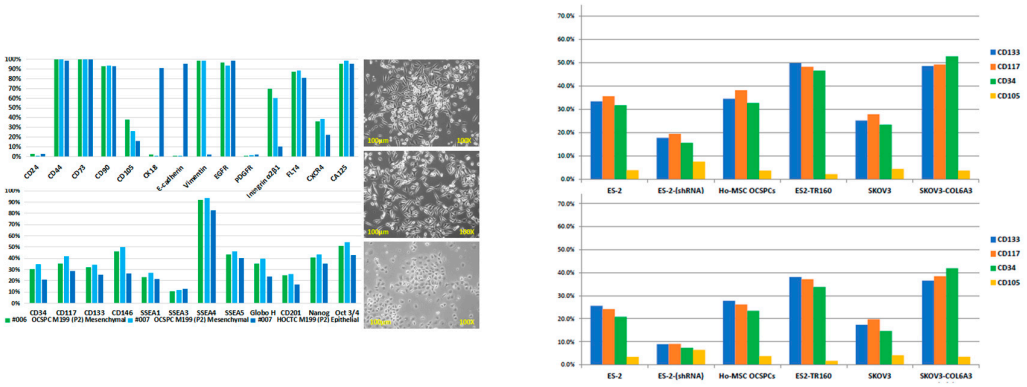

(**a**) (**b**)

Figure 1. Exosomes characterization of cell lines **(a)** (right) These are phase-contrast images of #006 and #007 human ovarian carcinoma.

ascites-derived cells (P2). The adherent culture condition is M199 +10%FBS + 20ng/mL EGF+ 0.4ug/mL hydrocortisone. (left) The surface expression markers of human ovarian carcinoma ascites and tissues derived cells with mesenchymal-like (MSC-) (right upper and middle) ovarian carcinoma stromal progenitor cells (OCSPCs) and epithelial-like (epi-) (right lower) ovarian carcinoma stromal progenitor cells from 2 advanced ovarian cancer patients. (left) The high expressions of vimentin in MSC-OCSPCs and CK18 and E-cadherin in epi-OCSPCs were noted. The high expression of CD44, CD73, CD90, FLT4, CA125, and SSEA4 was noted in both cells. **(b)** The percentage of positive stemness markers as CD133, CD117, CD34, and CD105 were consistent in ES2, ES2-COL6A3 shRNA, MSC-OCSPCs, ES2TR160, SKOV3, and SKOV3-COL6A3 cells (upper) and exosomes (EXs) (lower). ES2TR160 and SKOV3-COL6A3 processed the highest percentage of CD133, CD117, and CD34 stemness phenotypes in cells and exosomes.

2.2. Invasion Ability of EOC Cell Lines Derived Exosomes

We next examined if EOC EXs promote EOC invasion. Our results indicated the invasion ability was significantly greater in ES2 cells treated with ES2 EXs, ES2TR160 EXs, ES2 TS EXs, or ES2TR160TS EXs than those without EXs ($p<0.01$ for ES2 EXs and ES2TR160 EXs, $p<0.001$ for ES2 TS EXs and

 doi:10.20944/preprints202406.1228.v1

ES2TR160 TS EXs, respectively) (Figure 2). We next asked if different EOC cells and MSC-OCSPCs-derived EXs processed different enhancements of invasion ability. We compared the invasion ability of EXs with degrees of aggressive EOC cell lines, including SKOV3 (serous type, less aggressive), ES2, ES2 TS, ES2TR160, and ES2TR TS (clear cell type derived, more aggressive), and MSC-OCSPCs (obtained from advanced EOC patients with massive ascites cultured in selective conditional media). The invasion ability of ES2 is the greatest enhanced by ES2TR TS EXs than ES2, ES2 TS, or ES2TR EXs (Figure 2A, 2C). We further asked if the EXs from more aggressive EOC cells have different degrees of invasiveness in more aggressive and less aggressive EOC cells. Our results revealed that the invasion ability of ES2, ES2 TS, ES2TR160, and ES2TR160 TS EXs was greater on ES2 (more aggressive) cells than on SKOV3 cells (less aggressive) (Figure 2B, 2D).

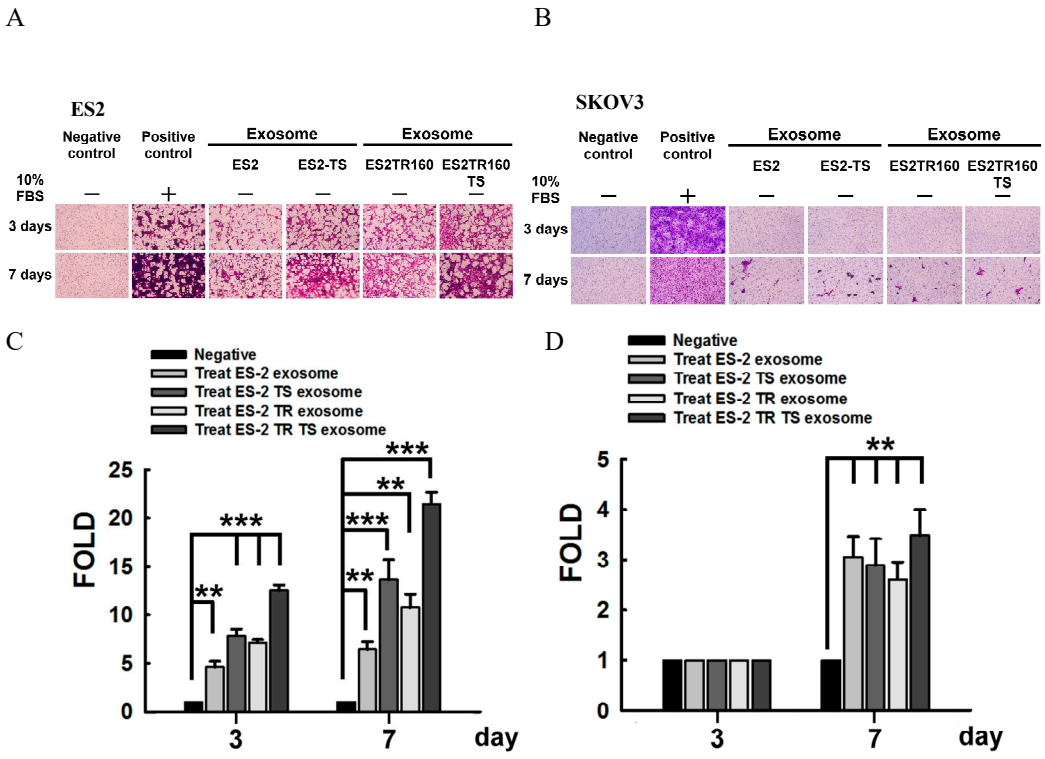

Figure 2. Invasion ability of EOC cell lines derived exosomes. The invasion ability was examined in ES2 **(A and C)** and SKOV3 **(B and D)** treated with and without ES2, ES2TR, ES2 tumor spheres, and ES2TR tumor spheres exosomes. The invasion ability of exosomes from ES2, ES2 TS, ES2TR, and ES2TR TS was remarkably enhanced in ES2 than in SKOV3 ($p<0.001$ for ES2, $P<0.01$ for SKOV3; respectively).

2.3. Invasion Ability of Autocrine and Paracrine Effects in EOC Cell Lines Derived Exosomes

We reasoned that the EOC EXs process both autocrine and paracrine effects to enhance invasiveness to EOC cells and MSC-OCSPCs in the microenvironment. We asked which type of OCSPCs could be increased by highly aggressive EOC cells derived EXs. The results showed that only MSC-OCSPCs could be enhanced by ES2-derived EXs ($p<0.01$) (Figure 3(a)). We next examined the paracrine effect of invasion ability in ES2 cells treated with MSC-OCSPC EXs or MSC-OCSPCs treated with ES2 EXs. The invasion ability was significantly greater in MSC-OCSPCs treated with ES2 EXs or ES2 cells treated with MSC-OCSPCs EXs than those without EXs ($p<0.001$, $p<0.01$; respectively). (Figure 3(b)). That implied EXs from cancer cells or MSC-OCSPCs could reciprocally promote invasiveness through the paracrine effect.

 doi:10.20944/preprints202406.1228.v1

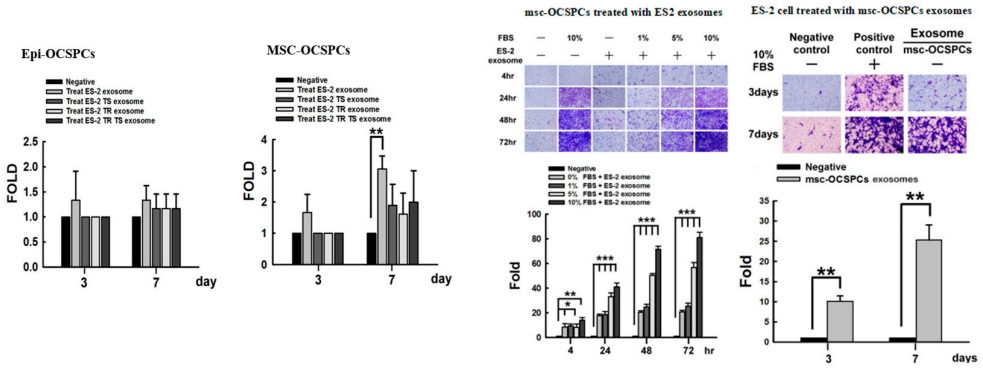

(**a**) (**b**)

Figure 3. Invasion ability of autocrine and paracrine effects in EOC cell lines derived exosomes. **(a)** The invasion ability was examined in epi-OCSPCs and MSC-OCSPCs treated with and without ES2, ES2TR, ES2 tumor spheres, and ES2TR tumor spheres exosomes. The invasion ability was only significantly enhanced in MSC-OCSPCs ($p<0.01$) treated with ES2 exosomes, but not in epi-OCSPCs. **(b)** The invasion ability was substantially increased in MSC-OCSPCs treated with than without ES2 exosomes ($p<0.001$). Simultaneously, the invasion ability was greater in ES2 cells treated with MSC-OCSPCs exosomes than those without MSC-OCSPCs exosomes ($p<0.01$).

2.4. Heat Map of Differential Expression of EOC Exosomes

We further asked which components of EXs from more aggressive ES2 cells enhanced invasion in EOC cells and MSC-OCSPCs. Using LC-MS/MS analyses, we compared the differential expression levels >2 among different groups in group 1: ES2 cells and ES2 EXs versus ES2 cells, group 2: ES2 with ES2 TS EXs versus ES2 cells, and group 3: MSC-OCSPCs and ES2 EXs versus MSC-OCSPCs. The results of the heat map are shown in Figure 4. COL6A3 was one of the statistically differential expression levels between Log2 (group 1 versus group 3):3.72 and Log2 (group 2 versus group 3):3.07. Our previous study showed that Collagen VI can accelerate tumor growth and metastasis in EOC [22]. Overexpression of COL6A3 in tumor cells can directly remodel their extracellular matrix (ECM). This change in the ECM helps develop drug resistance and metastasis in ovarian cancer [25]. Therefore, we speculated that COL6A3 transport through EXs may participate in drug resistance and metastasis.

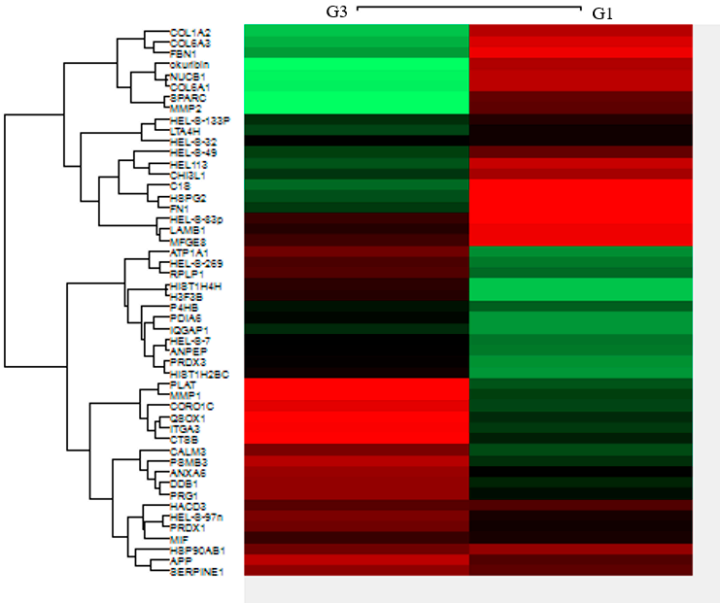

 doi:10.20944/preprints202406.1228.v1

Figure 4. Heat map of differential expression of EOC exosomes. The heat map shows group 1: ES2 cells and ES2 EXs versus ES2 cells and group 3: MSC-OCSPCs and ES2 EXs versus MSC-OCSPCs, using LC-MS/MS analyses.

2.5. COL6A3 Expression in EOC Cell Lines and Derived Exosomes

We first checked the expression level of collagen VI in more aggressive and less aggressive EOC cells and EXs. Our results showed Collagen VI (collagen alpha-3 (VI; COL6A3)) was present in more aggressive cells and EXs from ES2, ES2 TS, ES2TR, and ES2TR TS cells. In particular, the COL6A3 expressions were more prominent in ES2TR160 and ES2TR160 TS-derived EXs than ES2 and ES2 TS-derived EXs, which suggested COL6A3 EXs might participate in paclitaxel drug resistance. In contrast, Collagen VI was absent in less aggressive SKOV3 cells and EXs (Figure 5A and B). We next overexpressed COL6A3 in less aggressive SKOV3 cells (SKOV3/COL6A3) and knocked down COL6A3 in more aggressive ES2 cells (ES2/shCOL6A3). The results showed COL6A3 has expression in ES2, ES2 TS, and SKOV3/COL6A3 cells and those EXs; in contrast, COL6A3 has no expression in SKOV3 and ES2/shCOL6A3 cells and EXs in western blot analysis (Figure 5C). That implied COL6A3 has expression and secretion through the EXs route in more aggressive EOC cells and EOC TS cells but is not expressed and secreted in less aggressive EOC cells or more aggressive EOC knockdown COL6A3 cells and EXs. We further verified if COL6A3 protein has staining in ovarian tumor cells. COL6A3 was strong staining in cancerous stromal cells but without in cancer cells in high-grade serous ovarian carcinoma paraffin-embedded tissue by immunohistochemistry (Figure 5D). The result is consistent with no expression of COL6A3 in less aggressive SKOV3 cells (serous type). Our previous work showed COL6A3 highly expressed in MSC-OCSPC culture medium enhanced the invasiveness of SKOV3, while knockdown of COL6A3 in MSC-OCSPCs inhibited the invasiveness of EOC and spheroid [22]. In this study, COL6A3 has expression in more aggressive ES2, ES2 TS, ES2TR, ES2TR TS (clear cell type), and MSC-OCSPCs cells and those EXs (Figures 8A and B). We next examined the invasion ability of SKOV3 cells with or without SKOV3 EXs and SKOV3/COL6A3 cells with or without SKOV3/COL6A3 EXs. The invasion ability was significantly greater in SKOV3 cells with SKOV3 EXs and SKOV3/COL6A3 cells with SKOV3/COL6A3 EXs than those without EXs (both $p<0.001$).

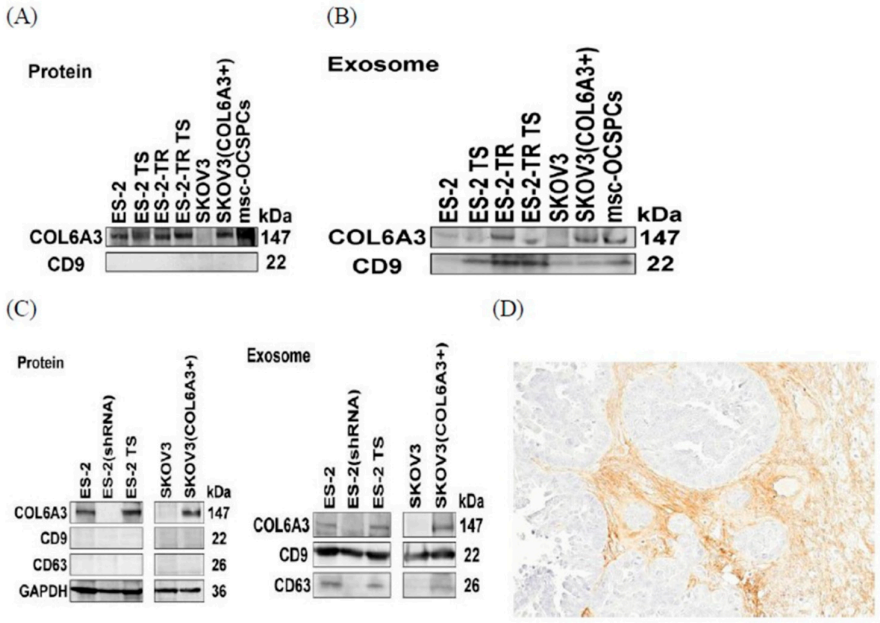

Figure 5. COL6A3 expression in EOC cell lines and derived exosomes. **(A)** and **(B)** COL6A3 was expressed in ES2 derivatives, SKOV3/COL6A3, and MSC-OCSPCs derived exosomes and lysates

 doi:10.20944/preprints202406.1228.v1

compared to no expression in SKOV3 and ES2/shRNA derived exosomes and cell lysates. **(C)** The CD9 and CD63 representative exosome markers were seen in ES2 derivative, SKOV3/COL6A3, and MSC-OCSPCs derived exosomes, but CD9 and CD63 were not detected in those cell lysates. **(D)** immunostaining of COL6A3 was positive staining in ovarian serous carcinoma stromal cells which surrounded cancer cells with negative staining.

2.6. The Invasion Ability of Overexpressed and Knockdown-EOC Cells with Those Exosomes

We next examined the invasion ability of SKOV3 cells with or without SKOV3 EXs and SKOV3/COL6A3 cells with or without SKOV3/COL6A3 EXs. The invasion ability was significantly greater in SKOV3 cells with SKOV3 EXs and SKOV3/COL6A3 cells with SKOV3/COL6A3 EXs than those without EXs (both $p<0.001$). Moreover, the invasion ability was greater in SKOV3/COL6A3 EXs with SKOV3/COL6A3 cells than in SKOV3/COL6A3 EXs with SKOV3 cells (Figure 6 A). Our results indicated that the ability of invasiveness enhanced by EOC-overexpressed COL6A3 EXs depends on varying degrees of aggressive malignant potential EOC cells. In contrast, the invasion ability was significantly inhibited in ES2/shCOL6A3 cells with ES2/shCOL6A3 EXs than in ES2 cells with ES2 EXs ($p<0.05$) (Figure 6C). However, the invasion ability was not significantly inhibited in ES2 cells with ES2/shCOL6A3 EXs than in ES2 cells with ES2 EXs (Figure 6B and D).

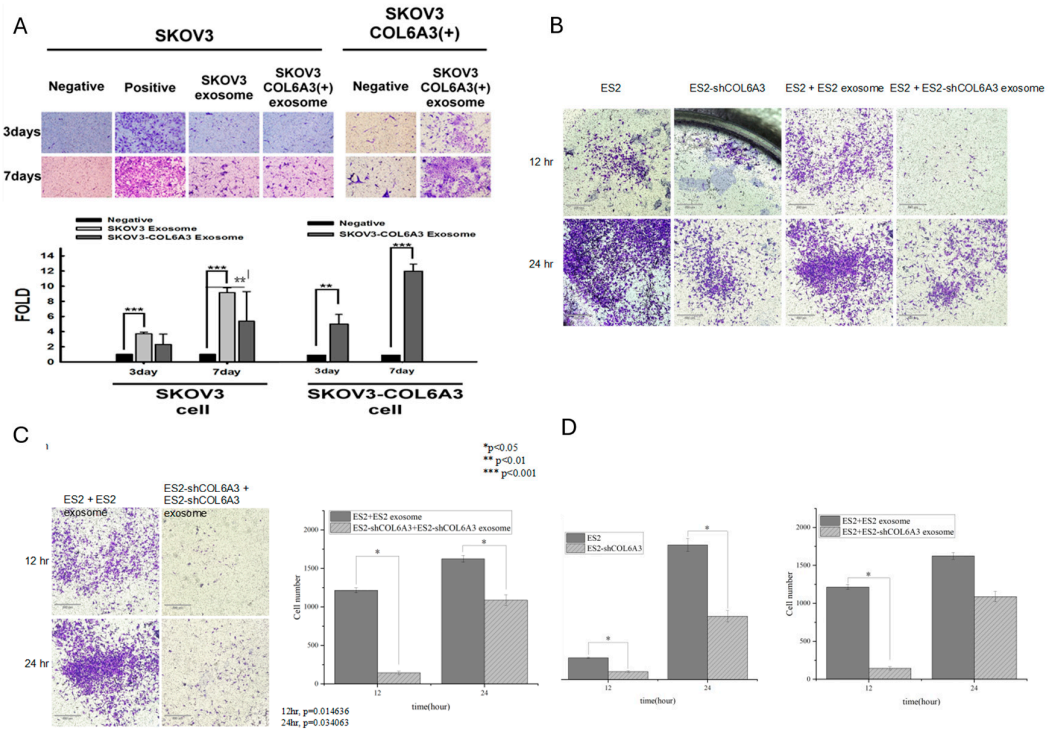

Figure 6. The invasion ability of overexpressed and knockdown-EOC cells with those exosomes **(A)** was examined in SKOV3 and SKOV3-COL6A3 cells treated with and without those respective EXs. The invasion ability was significantly greater in SKOV3 and SKOV3-COL6A3 cells treated with those respective EXs than those without EXs (both, $P<0.001$). **(B, C, and D)** The invasion ability was examined in ES2 and ES2 knockdown COL6A3 cells and EXs. The invasion ability was significantly greater in ES2 cells or with ES2 EXs than in ES2 knockdown COL6A3 cells or with EXs (both, $p<0.05$).

2.7. EOC-Derived EXs Accelerated Cancerous Peritoneal Dissemination

We reasoned that EOC-derived EXs could accelerate cancerous peritoneal dissemination and lung colonization. The data indicated that the EXs from ES2 cells, a rapidly disseminated cell line, possessed a higher invasion ability than the EXs from SKOV3 cells. Therefore, we examined whether ES2 EXs enhanced less aggressive EOC cells' peritoneal dissemination in vivo. To this end, luciferase-

 doi:10.20944/preprints202406.1228.v1

expressing SKOV3 cells, which displayed a less aggressive phenotype, were injected into the peritoneal cavity, and 10 μg of EXs from more aggressive ES2 cells or phosphate-buffered saline (PBS) were intraperitoneally injected twice weekly for 6 weeks. Six of the 7 mice intraperitoneally injected with 1×10^6 SKOV3 cells and ES2 EXs had a significantly greater disseminated burden in the peritoneal cavity compared with the 1 of 5 mice injected with 1×10^6 SKOV3 cells and PBS ($p = 0.023$, by the student's t-test). The average disseminated tumor numbers in the peritoneal cavity were greater in mice receiving SKOV3 cells with ES2 EXs than SKOV3 cells with PBS ($p<0.01$, by student's t-test) (Figure 7)

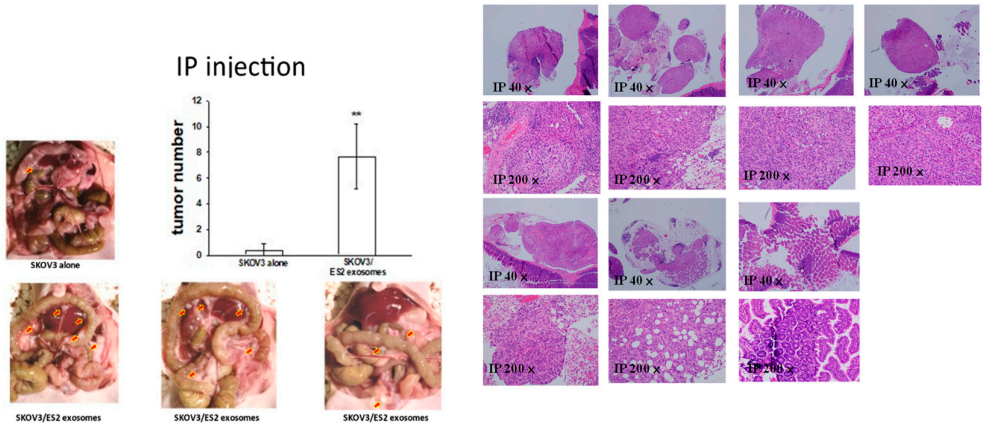

(**a**) (**b**)

Figure 7. EOC-derived EXs accelerated cancerous peritoneal dissemination. **(a)** The representative pictures of 6/7 mice IP injected 1×10^6 SKOV3 cells with ES2-exosomes had disseminated tumors in the peritoneal cavity compared to 1/3 mice injected 1×10^6 SKOV3 cells with PBS ($p=0.097$, by student's t-test). The average disseminated tumor numbers in the peritoneal cavity were significantly greater in mice receiving SKOV3 cells with ES2-exosomes than SKOV3 cells with PBS ($p<0.01$, by student's t-test). **(b)** The representative histologic pictures of disseminated peritoneal tumors were shown in microscopic 40X and 200X.

2.8. Overexpressed COL6A3 in EOC-Derived EXs Accelerated Cancerous Peritoneal Dissemination

Because COL6A3 has expression in ES2 EXs, which might enhance invasiveness and dissemination, we next reasoned whether COL6A3 is a key element for enhancing dissemination from ES2 EXs. We next overexpressed COL6A3 in SKOV3 cells (SKOV3/COL6A3) to see if COL6A3 accelerated peritoneal dissemination in vivo. To this end, $l\times10^6$ SKOV3/COL6A3 cells, presumed more aggressive cells, or $l\times10^6$ less aggressive SKOV3 cells were injected into the peritoneal cavity. Five of the 6 mice injected with 1×10^6 SKOV3/COL6A3 cells had a greater disseminated burden in the peritoneal cavity compared with one of the 5 mice injected with 1×10^6 SKOV3 cells ($p = 0.036$, by student's t-test). The average disseminated tumor numbers in the peritoneal cavity were significantly greater in mice receiving SKOV3/COL6A3 cells than SKOV3 cells ($p<0.001$, by student's t-test) (Figure 8).

 doi:10.20944/preprints202406.1228.v1

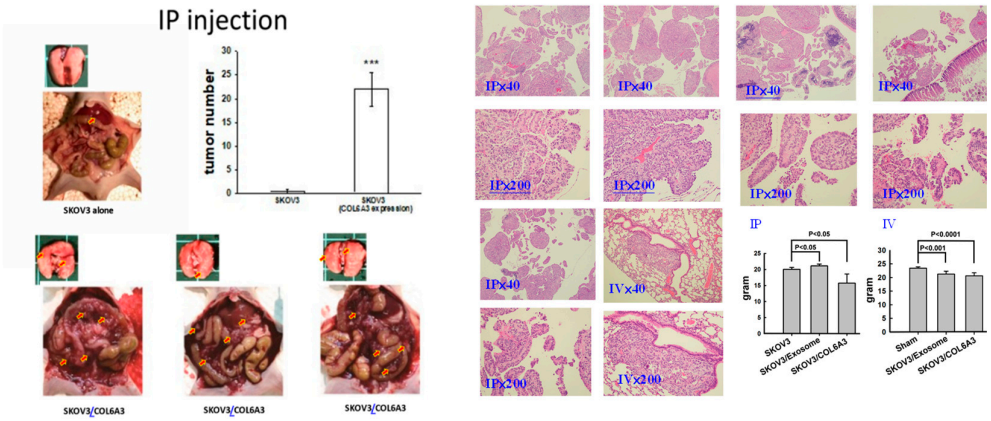

(**a**) (**b**)

Figure 8. Overexpressed COL6A3 in EOC-derived EXs accelerated cancerous peritoneal dissemination. **(a)** The representative pictures of average disseminated tumor numbers in the peritoneal cavity were significantly greater in mice receiving SKOV3 overexpressed COL6A3 (SKOV3/COL6A3) than in SKOV3 cells ($p<0.001$, by student's t-test). 1/8 mice IV injected 1×10^6 SKOV3/COL6A3 cells had colonization to lung compared to 0/32 mice injected 1×10^6 SKOV3 cells only ($p=0.043$, by student's t-test). **(b)** The representative histologic pictures of the peritoneal tumor and lung colonization were shown in microscopic 40X and 200X. The right lower panel showed the differential body weights of mice among IP and IV groups of SKOV3 cells, SKOV3 cells with ES2 exosomes, and SKOV3/COL6A3 cells.

2.9. Overexpressed COL6A3 in EOC-Derived EXs Accelerated Lung Colonization

We next examined whether SKOV3/COL6A3 cells also accelerated distant lung colonization in vivo. To this end, $l\times10^6$ SKOV3/COL6A3 cells or $l\times10^6$ SKOV3 cells were given intravenously into the tail vein in mice. One of 8 mice intravenously injected with 1×10^6 SKOV3/COL6A3 cells had colonization in the lung compared with 0 of 32 mice injected with 1×10^6 SKOV3 cells ($p = 0.043$, by student's t-test) (Figure 9). We next examined whether SKOV3/COL6A3 EXs help accelerate lung colonization in vivo. To this end, SKOV3/COL6A3 cells were intravenously injected with 10 μg of EXs from SKOV3/COL6A3 cells or phosphate-buffered saline (PBS) twice weekly for up to 10 weeks. Five of 8 mice intravenously injected with 1×10^6 SKOV3/COL6A3 cells and SKOV3/COL6A3 EXs had a significantly greater colonization burden in the lung compared with the 1 of 8 mice injected with 1×10^6 SKOV3/COL6A3 cells ($p=0.039$, by student's t-test) (Figure 9). These data suggest that COL6A3 and EXs processed more aggressive characteristics, which promotes EOC cell dissemination and colonization to the peritoneal cavity and lung. In contrast, knockdown of COL6A3 in EOC spheroids inhibited COL6A3 expression in EOC spheroids, which decreased EOC spheroid formation, invasion, tumor growth, and metastasis [28].

 doi:10.20944/preprints202406.1228.v1

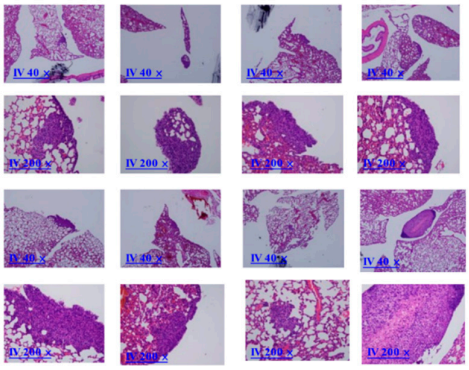

Figure 9. Overexpressed COL6A3 in EOC-derived EXs accelerated lung colonization. 5/8 mice IV injected 1×10^6 SKOV3/COL6A3 cells and 10μg SKOV3/COL6A3-exosomes had colonization to lung compared to 0/8 mice injected 1×10^6 SKOV3 cells and PBS (p=0.007, by student's t-test) and 1/8 mice IV injected 1×10^6 SKOV3/COL6A3 cells (p=0.039) (Figure 8(b)). The histologic pictures of lung colonization tumors were shown in microscopic 40X and 200X.

2.10. The Overall Survival of COL6A3 Expression

The OS for all subtypes and serous subtype EOC patients from GEO (n = 1656) and TCGA (n 1207) data with COL6A3 revealed significantly worse in the high expression group than in the low expression group (p = 0.0015 and p = 0.034, respectively) (Figure 10).

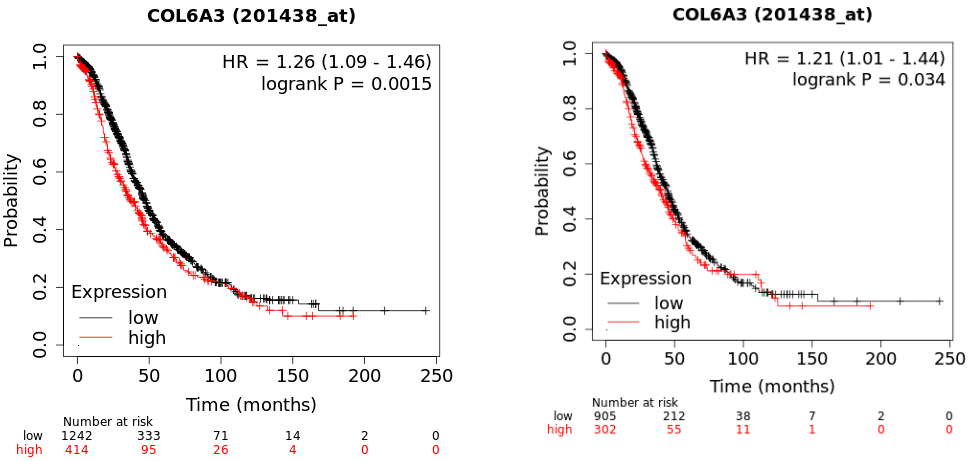

(**a**) (**b**)

Figure 10. The overall survival of COL6A3 expression. The overall survival of high expression of COL6A3 was significantly higher than those with low expression in **(a)** all subtypes and **(b)** serous subtypes of EOC patients from TCGA and GEO data.

2.11. GW4869 and Rampamycin Decreased Invasion Ability from EOC EXs

The invasion ability of ES2 cells treated with (a) GW4869 (10nM) or (b) rapamycin (500nM) was substantially reduced than in ES2 exosomes (p<0.01 for GW4869, p<0.001 for rapamycin; respectively) (Figure 11).

 doi:10.20944/preprints202406.1228.v1

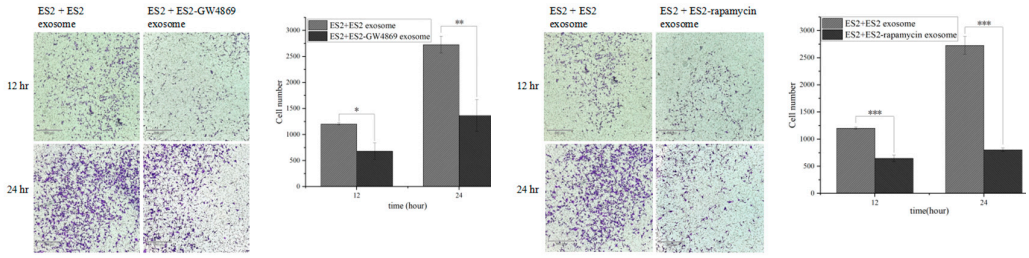

(**a**) (**b**)

Figure 11. GW4869 and Rapamycin decreased the invasion ability from EOC EXs. The invasion ability was inhibited in ES2 with ES2-treated with (a) GW4869 or (b) rapamycin exosomes than ES2 with ES2 exosomes.

3. Discussion

We first found COL6A3 exosomes promoting tumor dissemination and metastasis in epithelial ovarian cancer. Genetic knockdown COL6A3 or pharmacological inhibition of EXs release could abolish invasion and metastasis in EOC. In this study, high expressions of COL6A3 in EOC tissues associated with patients' survival status had a worse survival outcome than those of low expressions from TCGA and GEO data. The expression of COL6A3 was significantly higher in the ovarian tumor and metastatic omentum tissues in the advanced stage than in the early stage in our EOC patients [22]. Importantly, the COL6A3 was highly expressed in ES2 paclitaxel-resistant and ascites-derived MSC-OCSPCs cells and EXs. Ascites display aggressiveness and chemoresistance in ovarian cancer and lead to the dysregulation of lysosomal signaling, where lysosomes are critical for nutrient sensing and frequently associated with the rapamycin complex 1 (mTORC1) [30]. Lysosomal signaling involves energy demand for cancer cells in nutrient sensing [30]. Lysosomes are involved in the secretion of EX, and changes in lysosomal signaling and phenotype will also lead to changes in EX secretion [31], which has been implicated in cisplatin resistance. Autophagy can transport proteins through unconventional secretory pathways and carry cargo to lysosomes for degradation of organelles from fusion with lysosomes to the plasma membrane and secretes cargo from the cell [32]. Previous studies have shown that cancer cells release more EXs than non-malignant cells, making autophagy inhibitors decrease EX secretion a new anticancer therapy strategy [33]. The EXs biogenesis inhibitor GW4869 is the most widely used pharmacological agent to block EXs generation, reduce EXs release by nSMase inhibition, and reduce the number of EXs released. Inhibition of mTORC1 by **rapamycin,** a lysosome function enhancer, and an autophagy inducer, **also could inhibit exosomal release [34].**

Our previous studies show COL6A3 regulates the CDK4/6-pRb and AKT-mTOR pathways and promotes EOC stemness, invasion, and metastasis [22,28]. The combination of everolimus (mTOR inhibitor) and 5-aza-2-deoxycytidine (demethylating agent) can effectively inhibit the production of ovarian clear cell cancer stem-like/spheroid cells by inhibiting the COL6A3-AKT-mTOR pathway and generate anti-tumor effect [28]. In this study, we confirmed treatment with EXs inhibitor GW4869 or rapamycin-abolished including COL6A3-EXs may inhibit the aggressiveness in EOC. Limiting lysosomal exocytosis to reduce EX secretion may be an effective therapeutic strategy to reduce cancer cell invasiveness and chemoresistance [35].

Higher exosome-derived miR-200b and miR-200c concentrations in stage III-IV EOC patients have shortened OS [36]. EXs from EOC patients have higher concentrations of TGFB1, melanoma-associated antigen 3 (MAGE3), and MAGE6 [37]. EXs from EOC also have a higher concentration of Claudin 4 associated with tumor stage and CA125 levels [38]. EXs isolated from EOC plasma samples had higher CD24 and EpCAM [39]. Furthermore, over 2,000 proteins in EXs secreted from OVCAR-3 and IGROV1 ovarian cancer cell lines have been identified and are involved in tumorigenesis and

 doi:10.20944/preprints202406.1228.v1

metastasis to form the predictive potential of exosomal profiling [40]. However, more comprehensive clinical studies are needed to confirm the clinical value of this approach.

The cancer-associated fibroblasts (CAFs) can drive tumor proliferation, neo-vascularization, and invasion [41,42]. The tumor and the stroma reciprocal interactions establish a local microenvironment to accelerate tumor progression [43]. ECM molecules signaling to stromal and cancer cells increase or decrease cancer progression. Type VI collagen is in the base membrane and interstitial matrix interface. During tumor progression, CAFs are the major players in the dysregulated collagen cause of tumor fibrosis and excessive collagen depositions in the tumor [44,45]. Collagen stiffens tissues through crosslink and linearization and becomes fibroblast-derived stromal collagens which is directly correlated with the poorer survival outcome for the patients [46–50]. The exosomes from cancer cells through reprogramming or educating other cells prolong tumor survival and promote metastasis [51,52]. However, exosomes from the tumor microenvironments containing fibroblasts, mesothelial cells, adipocytes, and immune cells also affect cancer cells [53]. To this end, we performed pharmacological inhibition of nSMase2 and genetic knockdown COL6A3 decreasing exosomes. We confirmed that the COL6A3 secreting is from EOC cells and tumor stroma via the exosomal pathway to affect EOC cells and ascites derived-MSC-OCSPCs. The results indicate COL6A3 possesses established a premetastatic niche in the microenvironment.

Our data showed COL6A3 has expression in more aggressive ES2 derivatives, especially in ES2 paclitaxel-resistant cells and ascites-derived MSC-OCSPCs and those EXs, but not in less aggressive SKOV3 cells, ES2 knockdown COL6A3 (ES2/shCOL6A3) and those EXs. It is speculated that COL6A3 in more aggressive ES2 cells secreted from EXs route to remodeling ECM to affect ascites-derived stromal progenitor cells and establish a metastatic niche. However, COL6A3 expression in the differential responses of chemotherapy-naïve and relapsed EOC tissues will provide a better understanding of the potential of COL6 as a therapeutic target. COL6A3 secretion from the EXs route is an uncovered field in EOC progression and metastasis. As COL6A3 is essential in facilitating tumor progression and metastasis, future studies targeting COL6A3 as a valuable biomarker for early diagnosis of chemotherapy drug resistance, metastasis, recurrence, and prediction of survival outcome by checking COL6A3 exosome from blood, ascites, or tissues of EOC' patients, and mediated possible related signaling should be explored. It also holds promise for developing therapeutically targeting COL6-based conjugated antibodies or vaccines for EOC patients in the future.

4. Materials and Methods

4.1. Samples Collection

Ovarian Cancer tissues and discarded ascite samples obtained from surgery or symptom relief in patients with primary or recurrent ovarian cancer were immediately taken to the laboratory for processing. In vitro isolation and culture of OCSPCs from ascites and cancerous tissues were performed as described previously [26]. Cell lines and cultures (ES2 and SKOV3) were obtained from the American Type Culture Collection (ATCC). Cells were maintained in a humidified atmosphere containing 5% CO2 at 37 °C and grown in McCoy's 5A medium with 10% FBS. As previously described, we developed a paclitaxel-resistant ES2 cell line by continuously exposing cells to paclitaxel [27]. The final paclitaxel concentrations that induced paclitaxel-resistant subclones called ES2TR were 160 nM.

4.2. Tumor Sphere Formation of Ovarian Cancer Stem-Like Cells

ES2, ES2TR160, and ascites isolated from EOC patients were cultured in tumor sphere (spheroid)-inducing conditions to induce tumor sphere formation. Briefly, cells were cultured in DMEM/F12 medium with 20 ng/mL bFGF, 20 ng/mL EGF, 10 ng/mL IGF, and 2% B27 (Invitrogen, Carlsbad, CA). Dissociated single cells (1×10^5 cells/mL) were seeded into ultra-low attachment plates (Corning 3262, Pittston, PA). After 7 days, we counted the spheres formed with an Olympus light microscope (Olympus, Tokyo, Japan). Then, tumor spheres obtained after 14 days were harvested and analyzed with flow cytometry.

 doi:10.20944/preprints202406.1228.v1

4.3. ExoQuick-TC™

Biofluid was collected and centrifuged at 3000 × g for 15 minutes to remove cells and cell debris. The supernatant was transferred to a sterile vessel to add the appropriate volume of ExoQuick-TC to the biofluid. The well was mixed by inverting or flicking the tube, refrigerating overnight (at least 12 hours) at +4°C, and centrifuging the ExoQuick-TC/biofluid mixture at 1500 × g for 30 minutes. After centrifugation, the supernatant was aspirated. The residual ExoQuick-TC solution was spun down by centrifugation at 1500 × g for 5 minutes, and all fluid traces were removed by aspiration. Then resuspend the exosome pellet in 100-500 µl using sterile 1X PBS.

4.4. Nanoparticle Tracking Analysis

Purified exosomes were resuspended in 100 µL of 0.22 µm filtered PBS and analyzed using a NanoSight LM10 instrument (NanoSight, Salisbury, United Kingdom). The analysis was performed by applying a monochromatic 404 nm laser to dilute the exosomal preparation and measure the Brownian movements of each particle. The Nanoparticle Tracking Analysis software version 2.3 was used to analyze 60-second videos of data collection to give the mean, median, and mode of vesicle size and concentration.

4.5. Extracellular Exosomes (EXs) Flow Cytometry Analysis

EXs were incubated with biotinylated antibody-coated beads in 500 µl of bead wash buffer (System Biosciences, Inc.) overnight, in a 1.5 ml tube at 4°C. After the binding step, beads were stained with either anti-CD9, anti-CD34, anti-CD63, anti-CD81, anti-CD105, anti-CD117, or anti-CD133 antibodies (BD Biosciences), either biotinylated, APC, FITC, Pacific Blue, PE, or PE-Cy7 conjugated. After antibody binding, beads were washed with bead wash buffer and recovered using a magnetic stand (optional, cat# EXOFLOW700A-1). When using a biotinylated antibody, a step incubating with streptavidin-FITC (System Biosciences, Inc.) was added, followed by EXs stain buffer (System Biosciences, Inc.). Samples were analyzed using FACS LSRFortessa cytometers (BD Biosciences), and data were analyzed using FACS Diva or FlowJo (BD Biosciences).

4.6. COL6A3 Knockdown and Overexpression

The COL6A3 knockdown in MSC-OCSPCs and ES2 cells and overexpression in SKOV3 cells were described previously [22].

4.7. LC-MS/MS Analysis

Protein digestion and dimethyl labeling of peptides The condition mediums were reduced with 10mM dithiothreitol, alkylated with 50mM iodoacetamide, and digested with Lys-C and trypsin. The digested peptides were labeled with isotopic formaldehyde (13CD2O, heavy labeled) and formaldehyde (CH2O, light labeled), respectively. Equal amounts of the heavy and light labeled peptides were mixed and desalted with StageTips with Empore™ SDB-CX disc membrane (3M, St. Paul, MN, USA).

NanoLC-MS/MS analyses. The peptides were analyzed using nanoLC-MS/MS on an online Dionex 3000 RSLC nanosystem (Thermo Fisher Scientific) coupled to an LTQ Orbitrap XL mass spectrometer (Thermo Fisher Scientific). SpeedVac dried the supernatant. Redissolved peptides with 0.5% acetic acid and 2% acetonitrile (ACN) and loaded onto an in-house-prepared 100µm×15cm tip column, were packed with 3µm ReproSil-Pur 120 C18-AQ reverse-phase beads and eluted at a flow rate of 500 nL/min. The mobile phases used for nanoLC will be 0.5% acetic acid in water (buffer A) and a mixture of 0.5% acetic acid and 80% ACN (buffer B). The LC gradient conditions were 5% to 40% buffer B in 60 min, 40% to 100% buffer B in 5 min, and 100% buffer B in 10 min. The LTQ Orbitrap XL system was operated in the positive ion mode and full-scan MS spectra (m/z 300-1600) were acquired on the Orbitrap analyzer with a resolution of 60000 at m/z 400. Raw files from LC-MS/MS were analyzed using the MaxQuant software. The differential expression levels were compared among different groups in group 1: ES2 cells and ES2 EXs versus ES2 cells, group 2: ES2 with ES2 TS

 doi:10.20944/preprints202406.1228.v1

EXs versus ES2 cells, and group 3: MSC-OCSPCs and ES2 EXs versus MSC-OCSPCs. The cutoff value was defined as the differential expression level>2.

4.8. Analysis of TCGA and GEO Data

We downloaded 372 TCGA OV RNA-Seq level 3 read count data (serous type) from the GDC Data Portal (https://portal.gdc.cancer.gov/). The gene annotation file was used in GENCODE version 22 and obtained from GDC Reference Files (https://gdc.cancer.gov/about-data/gdc-data-processing/gdc-reference-files), which the TCGA program used. Clinical follow-up information was found in the PanCanAtlas publication (https://gdc.cancer.gov/about-data/publications/pancanatlas). We calculated the best cut-off by splitting patients into high and low expression, which was an autoselect, and computed all possible cutoff values between the lower and upper quartiles, and the best-performing threshold was used as a cutoff. Microarray data from GEO and TCGA for all subtypes and RNA-seq data from the TCGA data set for all subtypes and serous types were used for survival analysis. The survival curve was plotted by overall survival (OS) and progression-free survival (PFS) from 1656 and 1435 patients for GEO and TCGA data and 373 and 177 patients for TCGA data.

4.9. Invasion Experiments

For invasion assays, we used transwell chambers (8 μm, 24-well format; Corning Inc., Corning, NY, USA) or Matrigel-coated transwell chambers (BD Biosciences, San Jose, CA, USA) that were inserted into 24-well cell culture plates. SKOV3 cells, ES2 cells, or MSC-OCSPCs, (5× 10^4 cells in 0.2 mL of serum-free medium) were added to the upper chamber, and culture medium (McCoy's 5A medium) in the lower chamber with a serum-free condition for the negative control, or containing 10% FBS for the positive control, or added culture medium (McCoy's 5A medium) with a serum-free condition and treating EXs (30ug) from SKOV3, SKOV3/COL6A3, ES2, ES2/shCOL6A3, ES2 TS, ES2TR, S2TR TS, CSPCs, MSC-OCSPCs/shCOL6A3 or ES2 cells treated with GW4869 or rampamycin cell extracts. Cells were cultured for 1, 3 days, or 7 days, and cells that invaded the inserts were fixed in methanol for 20 min, stained with crystal violet, and counted in three random microscope fields (Olympus BX3, Olympus, Tokyo, Japan) at a magnification of 40×, 100×, or 200×.

4.10. Western Blot Analysis

Cells were lysed in phosphate-buffered saline (PBS) containing 1% Triton X-100 using an ultrasonic cell disruptor. Lysates were separated using SDS-PAGE (12.5%) and transferred to a polyvinylidene fluoride membrane (NEN). The membranes were blocked in blocking buffer (tris-buffered saline containing 0.2% Tween 20 and 1% I-block [NEN]) and incubated with polyclonal antibodies (Ab) separately for 1 h. A purified rabbit antihuman GAPDH polyclonal Ab (Santa Cruz Biotechnology, Inc., Dallas, TX, USA) was applied simultaneously to normalize the signals generated from the anti-COL6A3, CD9, and CD63 (Cell Signaling). After washing, an alkaline phosphatase-conjugated anti-rabbit antibody (Vector Laboratories, Burlingame, CA, USA) was applied. The membranes were washed, and the bound Abs were visualized by developing the nitro blue tetrazolium/5-bromo-4-chloro-3-indolyl phosphate chromogen.

4.11. In Vivo Animal Experiments and Tumor Imaging

Female null mice (BALB/cAnN.Cg-Foxn1nu/CrlNarl) were purchased from the National Animal Center (Taipei, Taiwan), and the Institutional Animal Care and Use Committee of Cathay General Hospital approved all experiments. In experimental 1, null mice at 5-7 weeks of age (5 mice/group) were injected intraperitoneally with luciferase-expressing SKOV3 cells, which displayed a less aggressive phenotype, were injected into the peritoneal cavity, and 10 μg of EXs from more aggressive ES2 cells or phosphate-buffered saline (PBS) were intraperitoneally injected twice weekly for 6 weeks. In experimental 2, null mice at 5-7 weeks of age (5 mice/group) were injected intraperitoneally with l×10^6 SKOV3/COL6A3 cells, which displayed a more aggressive phenotype, or

 doi:10.20944/preprints202406.1228.v1

l×10^6 less aggressive SKOV3 cells were injected into the peritoneal cavity. In experimental 3, l×10^6 SKOV3/COL6A3 cells or l×10^6 SKOV3 cells were given intravenously into the tail vein in mice. In experimental 4, SKOV3/COL6A3 cells were intravenously injected with 10 μg of EXs from SKOV3/COL6A3 cells or phosphate-buffered saline (PBS) twice weekly for up to 10 weeks to examine the tumor dissemination and growth. The body weight of mice was measured, recorded, and compared with the body change every week. The number and size of metastatic tumor nodules in mice were recorded and measured when mice were sacrificed. Disseminated tumor numbers were measured and counted using calipers, and volumes were calculated based on the modified ellipsoid formula (L × W × W/2). Tumor weights were measured following euthanasia at the endpoint. The histologic examination of tumor growth in the peritoneal cavity and lung was confirmed during H&E stains for diagnosis.

4.12. Statistical Analysis.

Data were analyzed using SPSS 16.0 (SPSS Inc., Chicago, IL, USA). All numerical data are expressed as the mean ± SD from at least three experiments. Significant differences between the two groups were determined using Student's t-test, and important differences among more than two groups will be determined using a one-way ANOVA. Progression-free survival (PFS) and OS were calculated through the Kaplan-Meier method. Differences in survival curves were calculated using the log-rank test. $p < 0.05$ was considered statistically significant. P^* represents $p<0.05$, p^{**} represents $p<0.01$, p^{***} represents $p<0.001$.

Author Contributions: Conceptualization: CM.H., methodology: CM.H., TL.Y., TH.C., SH.H.; validation: TH.C, SH.H., formal analysis: TH.C. and CM.H; investigation and data curation: CM.H. and TL.Y.; first draft writing: CM.H., critics and improvements of the manuscript: CM.H TL.Y; review and editing: CM.H; supervision: TH.C. and SH.H. project administration: CM.H.; funding acquisition: CM.H. All authors have read and agreed to the published version of the manuscript.

Funding: This work was supported by research funds from the National Science Council, Taiwan (107-2314-B-281-005-MY3, 111-2314-B-281-008-MY3).

Institutional Review Board Statement: The institutional review board of Cathay General Hospital (CGH) approved this study (CGH-P110093). The study was conducted following the Declaration of Helsinki, and approved by the Institutional Review Board of Cathay General Hospital (CGH) (protocol code CGH-P110093).

Institutional Animal Care and Use Committee Statement: The Institutional Animal Care and Use Committee of the Cathay General Hospital approved this study (CGH-IACUC-111-003)

Informed Consent Statement: Informed consent was obtained from all subjects involved in the study.

Conflicts of Interest: The authors declare no conflicts of interest.

References

1. Siegel, R.L.; Miller, K.D.; Jemal, A. Cancer statistics, 2019. *CA Cancer J. Clin.* **2019**, *69*, 7-34.
2. Webb, P.M.; Jordan, S.J. Epidemiology of epithelial ovarian cancer. *Best Pract. Res. Clin. Obstet. Gynaecol.* **2017**, *41*, 3-14.
3. Kurman, R.J.; Shih, I.M. The dualistic model of ovarian carcinogenesis: revisited, revised, and expanded. *Am. J. Pathol.* **2016**, *186*, 733-747.
4. Cho, K.R.; Shih, I.M. Ovarian cancer. *Annu. Rev. Pathol.* **2009**, *4*, 287-313.
5. Kipps, E.; Tan, D.S.P.; Kaye, S.B. Meeting the challenge of ascites in ovarian cancer: new avenues for therapy and research. *Nat. Rev. Cancer* **2013**, *13*, 273-282.
6. Ahmed, N.; Stenvers, K.L. Getting to know ovarian cancer ascites: opportunities for targeted therapy-based translational research. *Front. Oncol.* **2013**, *3*, 256-258.
7. Lobb, R.J.; Lima, L.G.; Möller, A. Exosomes: key mediators of metastasis and premetastatic niche formation. *Semin. Cell Dev. Biol.* **2017**, *67*, 3-10.
8. Zhou, L.; Lv, T.; Zhang, Q.; Zhu, Q.; Zhan, P.; Zhu, S.; Zhang, J.; Song, Y. The biology, function and clinical implications of exosomes in lung cancer. *Cancer Lett.* **2017**, *407*, 84-92.
9. Aghabozorgi, A.S.; Ahangari, N.; Eftekhaari, T.E.; Torbati, P.N.; Bahiraee, A.; Ebrahimi, R.; Pasdar, A. Circulating exosomal miRNAs in cardiovascular disease pathogenesis: new emerging hopes. *J. Cell. Physiol.* **2019**, *234*, 21796-21809.

 doi:10.20944/preprints202406.1228.v1

10. Kim, H.; Lee, S.; Shin, E.; Seong, K.M.; Jin, Y.W.; Youn, H.; Youn, B. The emerging roles of exosomes as EMT regulators in cancer. *Cells* **2020**, *9*, 861.
11. Zeng, Z.; Li, Y.; Pan, Y.; Lan, X.; Song, F.; Sun, J.; Zhou, K.; Liu, X.; Ren, X.; Wang, F.; Hu, J.; Zhu, X.; Yang, W.; Liao, W.; Li, G.; Ding, Y.; Liang, L. Cancer-derived exosomal miR-25-3p promotes pre-metastatic niche formation by inducing vascular permeability and angiogenesis. *Nat. Commun.* **2018**, *9*, 1-14.
12. Zhang, D.; Li, D.; Shen, L.; Hu, D.; Tang, B.; Guo, W.; Wang, Z.; Zhang, Z.; Wei, G.; He, D. Exosomes derived from Piwil2-induced cancer stem cells transform fibroblasts into cancer-associated fibroblasts. *Oncol. Rep.* **2020**, *43*, 1125-1132.
13. Lobb, R.J.; Lima, L.G.; Möller, A. Exosomes: key mediators of metastasis and premetastatic niche formation. *Semin. Cell Dev. Biol.* **2017**, *67*, 3-10.
14. Nakamura, K.; Sawada, K.; Kinose, Y.; Yoshimura, A.; Toda, A.; Nakatsuka, E.; Hashimoto, K.; Mabuchi, S.; Morishige, K.I.; Kurachi, H.; Lengyel, E.; Kimura, T. Exosomes promote ovarian cancer cell invasion through the transfer of CD44 to peritoneal mesothelial cells. *Mol. Cancer Res.* **2017**, *15*, 78-92.
15. Yokoi, A.; Yoshioka, Y.; Yamamoto, Y.; Ishikawa, M.; Ikeda, S.I.; Kato, T.; Kiyono, T.; Takeshita, F.; Kajiyama, H.; Kikkawa, F.; Ochiya, T. Malignant extracellular vesicles carrying MMP1 mRNA facilitate peritoneal dissemination in ovarian cancer. *Nat. Commun.* **2017**, *6*, 14470.
16. Cho, J.A.; Park, H.; Lim, E.H.; Kim, K.H.; Choi, J.S.; Lee, J.H.; Shin, J.W.; Lee, K.W. Exosomes from ovarian cancer cells induce adipose tissue-derived mesenchymal stem cells to acquire the physical and functional characteristics of tumor-supporting myofibroblasts. *Gynecol. Oncol.* **2011**, *123*, 379-386.
17. Giusti, I.; D'Ascenzo, S.; Dolo, V. Ovarian cancer-derived extracellular vesicles affect normal human fibroblast behavior. *Cancer Biol. Ther.* **2018**, *19*, 722-734.
18. Lee, A.H.; Ghosh, D.; Quach, N.; Schroeder, D.; Dawson, M.R. Ovarian cancer exosomes trigger a differential biophysical response in tumor-derived fibroblasts. *Sci. Rep.* **2020**, *10*, 8686.
19. Yoshihara, M.; Kajiyama, H.; Yokoi, A.; Sugiyama, M.; Koya, Y.; Yamakita, Y.; Liu, W.; Nakamura, K.; Moriyama, Y.; Yasui, H.; Suzuki, S.; Yamamoto, Y.; Ricciardelli, C.; Nawa, A.; Shibata, K.; Kikkawa, F. Ovarian cancer-associated mesothelial cells induce acquired platinum resistance in peritoneal metastasis via the FN1/Akt signaling pathway. *Int. J. Cancer* **2020**, *46*, 2268-2280.
20. Clarke, C.J.; Berg, T.J.; Birch, J.; Ennis, D.; Mitchell, L.; Cloix, C.; Campbell, A.; Sumpton, D.; Nixon, C.; Campbell, K.; Bridgeman, V.L.; Vermeulen, P.B.; Foo, S.; Kostaras, E.; Jones, J.L.; Haywood, L.; Pulleine, E.; Yin, H.; Strathdee, D.; Sansom, O.; Blyth, K.; McNeish, I.; Zanivan, S.; Reynolds, A.R.; Norman, J.C. The initiator methionine tRNA drives secretion of type II collagen from stromal fibroblasts to promote tumor growth and angiogenesis. *Curr. Biol.* **2016**, *26*, 755-765.
21. Chen, P.; Cescon, M.; Bonaldo, P. Collagen VI in cancer and its biological mechanisms. *Trends Mol. Med.* **2013**, *19*, 410-417.
22. Ho, C.M.; Chang, T.H.; Yen, T.L.; Hong, K.J.; Huang, S.H. Collagen type VI regulates the CDK4/6-p-Rb signaling pathway and promotes ovarian cancer invasiveness, stemness, and metastasis. *Am. J. Cancer Res.* **2021**, *11*, 668-690.
23. Sherman-Baust, C.A.; Weeraratna, A.T.; Rangel, L.B.A.; Pizer, E.S.; Cho, K.R.; Schwartz, D.R.; Shock, T.; Morin, P.J. Remodeling of the extracellular matrix through overexpression of collagen VI contributes to cisplatin resistance in ovarian cancer cells. *Cancer Cell* **2003**, *3*, 377-386.
24. Pietilä, E.A.; Gonzalez-Molina, J.; Moyano-Galceran, L.; Jamalzadeh, S.; Zhang, K.; Lehtinen, L.; Turunen, S.P.; Martins, T.A.; Gultekin, O.; Lamminen, T.; Kaipio, K.; Joneborg, U.; Hynninen, J.; Hietanen, S.; Grénman, S.; Lehtonen, R.; Hautaniemi, S.; Carpén, O.; Carlson, J.W.; Lehti, K. Co-evolution of matrisome and adaptive adhesion dynamics drives ovarian cancer chemoresistance. *Nat. Commun.* **2021**, *12*, 3904.
25. Xu, S.; Xu, H.; Wang, W.; Li, S.; Li, H.; Li, T.; Zhang, W.; Yu, X.; Liu, L. The role of collagen in cancer: from bench to bedside. *J. Transl. Med.* **2019**, *17*, 309.
26. Ho, C.M.; Chang, S.F.; Hsiao, C.C.; Chien, T.Y.; Shih, D.T. Isolation and characterization of stromal progenitor cells from ascites of patients with epithelial ovarian adenocarcinoma. *J. Biomed. Sci.* **2012**, *14*, 19-23.
27. Ho, C.M.; Huang, C.J.; Huang, S.H.; Chang, S.F.; Cheng, W.F. Demethylation of HIN-1 reverses paclitaxel-resistance of ovarian clear cell carcinoma through the AKT-mTOR signaling pathway. *BMC Cancer* **2015**, *15*, 789.
28. Ho, C.M.; Lee, F.K.; Yen, T.L.; Huang, S.H.; Cheng, W.F. Everolimus Combined with 5-aza-2-deoxycytidine Generated Potent Anti-tumor Effects on Ovarian Clear Cell Cancer Stem-like/spheroid Cells by Inhibiting the COL6A3-AKT-mTOR Pathway. *Am. J. Cancer Res.* **2022**, *12*, 1686-1706.
29. Ho, C.M.; Shih, D.T.; Hsiao, C.C.; Huang, S.H.; Chang, S.F.; Cheng, W.F. Gene methylation of human ovarian carcinoma stromal progenitor cells promotes tumorigenesis. *J. Transl. Med.* **2015**, *13*, 367
30. Machado, E.; White-Gilbertson, S.; van de Vlekkert, D.; Janke, L.; Moshiach, S.; Campos, Y.; Finkelstein, D.; Gomero, E.; Mosca, R.; Qiu, X.; Morton, C.L.; Annunziata, I.; d'Azzo, A. Regulated lysosomal exocytosis mediates cancer progression. *Sci. Adv.* **2015**, *1*, e1500603.

31. González, A.; Hall, M.N. Nutrient sensing and TOR signaling in yeast and mammals. *EMBO J.* **2017**, *36*, 397-408.
32. Buratta, S.; Tancini, B.; Sagini, K.; Delo, F.; Chiaradia, E.; Urbanelli, L.; Emiliani, C. Lysosomal Exocytosis, Exosome Release and Secretory Autophagy: The autophagic- and endo-lysosomal systems go extracellular. *Int. J. Mol. Sci.* **2020**, *21*, 2576.
33. Raudenska, M.; Bavan, J.; Masarik, M. Crosstalk between autophagy inhibitors and endosome-related secretory pathways: a challenge for autophagy-based treatment of solid cancers. *Mol. Cancer* **2021**, *20*, 140.
34. Han, Q.F.; Li, W.J.; Hu, K.S.; Gao, J.; Zhai, W.L.; Yang, J.H.; Zhang, S.J. Exosome biogenesis: machinery, regulation, and therapeutic implications in cancer. *Mol. Cancer* **2022**, *21*, 207.
35. Pietila, E.A.; Gonzalez-Molina, J.; Moyano-Galceran, L.; Jamalzadeh, S.; Zhang, K.; Lehtinen, L.; Turunen, S.P.; Martins, T.A.; Gultekin, O.; Lamminen, T.; Kaipio, K.; Joneborg, U.; Hynninen, J.; Hietanen, S.; Grénman, S.; Lehtonen, R.; Hautaniemi, S.; Carpén, O.; Carlson, J.W.; Lehti, K. Coevolution of matrisome and adaptive adhesion dynamics drives ovarian cancer chemoresistance. *Nat. Commun.* **2021**, *12*, 3904.
36. Meng, X.; Müller, V.; Milde-Langosch, K.; Trillsch, F.; Pantel, K.; Schwarzenbach, H. Diagnostic and prognostic relevance of circulating exosomal miR-373, miR-200a, miR-200b and miR-200c in patients with epithelial ovarian cancer. *Oncotarget* **2016**, *13*, 16923-16935.
37. Szajnik, M.; Derbis, M.; Lach, M.; Patalas, P.; Michalak, M.; Drzewiecka, H.; Szpurek, D.; Nowakowski, A.; Spaczynski, M.; Baranowski, W.; Whiteside, T.L. Exosomes in Plasma of Patients with Ovarian Carcinoma: Potential Biomarkers of Tumor Progression and Response to Therapy. *Gynecol. Obstet.* (Sunnyvale) **2013**, Suppl. 4, 3.
38. Li, J.; Sherman-Baust, C.A.; Tsai-Turton, M.; Bristow, R.E.; Roden, R.B.; Morin, P.J. Claudin-containing exosomes in the peripheral circulation of women with ovarian cancer. *BMC Cancer* **2009**, *9*, 244.
39. Zhao, Z.; Yang, Y.; Zeng, Y.; He, M. A microfluidic ExoSearch chip for multiplexed exosome detection towards blood-based ovarian cancer diagnosis. *Lab Chip* **2016**, *16*, 489-496.
40. Liang, B.; Peng, P.; Chen, S.; Li, L.; Zhang, M.; Cao, D.; Yang, J.; Li, H.; Gui, T.; Li, X.; Shen, K. Characterization and proteomic analysis of ovarian cancer-derived exosomes. *J. Proteomics* **2013**, *80*, 171-182.
41. Kalluri, R. The biology and function of fibroblasts in cancer. *Nat. Rev. Cancer* **2016**, *16*, 582-598.
42. Kalluri, R.; Zeisberg, M. Fibroblasts in cancer. *Nat. Rev. Cancer* **2006**, *6*, 392-401.
43. Pankova, D.; Chen, Y.; Terajima, M.; Schliekelman, M.J.; Baird, B.N.; Fahrenholtz, M.; Sun, L.; Gill, B.J.; Vadakkan, T.J.; Kim, M.P.; Ahn, Y.H.; Roybal, J.D.; Liu, X.; Parra Cuentas, E.R.; Rodriguez, J.; Wistuba, I.I.; Creighton, C.J.; Gibbons, D.L.; Hicks, J.M.; Dickinson, M.E.; West, J.L.; Grande-Allen, K.J.; Hanash, S.M.; Yamauchi, M.; Kurie, J.M. Cancer-associated fibroblasts induce a collagen cross-link switch in tumor stroma. *Mol. Cancer Res.* **2016**, *14*, 287-295.
44. Sasser, K.; Hall, B. Encyclopedia of Cancer, Desmoplasia [internet]; 2011. Available from: https://doi.org/10.1007/978-3-662-46875-3.
45. Bager, C.L.; Willumsen, N.; Leeming, D.J.; Smith, V.; Karsdal, M.A.; Dornan, D.; Bay-Jensen, A.C. Collagen degradation products measured in serum can separate ovarian and breast cancer patients from healthy controls: a preliminary study. *Cancer Biomarkers* **2015**, *15*, 783-788.
46. Willumsen, N.; Bager, C.L.; Leeming, D.J.; Smith, V.; Karsdal, M.A.; Dornan, D.; Bay-Jensen, A.C. Extracellular matrix specific protein fingerprints measured in serum can separate pancreatic cancer patients from healthy controls. *BMC Cancer* **2013**, *13*, 554.
47. Willumsen, N.; Bager, C.L.; Leeming, D.J.; Smith, V.; Christiansen, C.; Karsdal, M.A.; Dornan, D.; Bay-Jensen, A.C. Serum biomarkers reflecting specific tumor tissue remodeling processes are valuable diagnostic tools for lung cancer. *Cancer Med.* **2014**, *3*, 1136-1145.
48. Kehlet, S.N.; Sanz-Pamplona, R.; Brix, S.; Leeming, D.J.; Karsdal, M.A.; Moreno, V. Excessive collagen turnover products are released during colorectal cancer progression and elevated in serum from metastatic colorectal cancer patients. *Sci. Rep.* **2016**, *6*, 1-7.
49. Leeming, D.J.; Koizumi, M.; Qvist, P.; Barkholt, V.; Zhang, C.; Henriksen, K.; Byrjalsen, I.; Karsdal, M.A. Serum N-Terminal Propeptide of Collagen Type I is Associated with the Number of Bone Metastases in Breast and Prostate Cancer and Correlates to Other Bone Related Markers. *Biomark. Cancer* **2011**, *3*, 15-23.
50. Peinado, H.; Alečković, M.; Lavotshkin, S.; Matei, I.; Costa-Silva, B.; Moreno-Bueno, G.; Hergueta-Redondo, M.; Williams, C.; Garcia-Santos, G.; Ghajar, C.; Nitadori-Hoshino, A.; Hoffman, C.; Badal, K.; Garcia, B.A.; Callahan, M.K.; Yuan, J.; Martins, V.R.; Skog, J.; Kaplan, R.N.; Brady, M.S.; Wolchok, J.D.; Chapman, P.B.; Kang, Y.; Bromberg, J.; Lyden, D. Melanoma exosomes educate bone marrow progenitor cells toward a pro-metastatic phenotype through MET. *Nat. Med.* **2012**, *18*, 883-891.
51. Zhou, W.; Fong, M.Y.; Min, Y.; Somlo, G.; Liu, L.; Palomares, M.R.; Yu, Y.; Chow, A.; O'Connor, S.T.; Chin, A.R.; Yen, Y.; Wang, Y.; Marcusson, E.G.; Chu, P.; Wu, J.; Wu, X.; Li, A.X.; Li, Z.; Gao, H.; Ren, X.; Boldin, M.P.; Lin, P.C.; Wang, S.E. Cancer-secreted miR-105 destroys vascular endothelial barriers to promote metastasis. *Cancer Cell* **2014**, *25*, 501-515.

 doi:10.20944/preprints202406.1228.v1

52. Zhao, H.; Yang, L.; Baddour, J.; Achreja, A.; Bernard, V.; Moss, T.; Marini, J.C.; Tudawe, T.; Seviour, E.G.; San Lucas, F.A.; Alvarez, H.; Gupta, S.; Maiti, S.N.; Cooper, L.; Peehl, D.; Ram, P.T.; Maitra, A.; Nagrath, D. Tumor microenvironment derived exosomes pleiotropically modulate cancer cell metabolism. *eLife* **2016**, *5*, e10250.
53. Tallon, C.; Hollinger, K.R.; Pal, A.; Bell, B.J.; Rais, R.; Tsukamoto, T.; Witwer, K.W.; Haughey, N.J.; Slusher, B.S. Nipping disease in the bud: nSMase2 inhibitors as therapeutics in extracellular vesicle-mediated diseases. *Drug Discov. Today* **2021**, *26*, 1656-1668.